Cooling Performance Analysis of Water-Cooled Heat Sinks with Circular and Rectangular Minichannels Using Finite Volume Method

Ghasemi, Seyed Ebrahim*[+]; Ranjbar, Ali Akbar

Department of Mechanical Engineering, Babol University of Technology, P.O. Box 484, Babol, I.R. IRAN

Hosseini, Seiyed Mohammad Javad

Department of Mechanical Engineering, Golestan University, P.O. Box 155, Gorgan, I.R. IRAN

ABSTRACT: *In this paper, the cooling performance of water-cooled heat sinks for heat dissipation from electronic components is investigated numerically. Computational Fluid Dynamics (CFD) simulations are carried out to study the rectangular and circular cross-sectional shaped heat sinks.The sectional geometry of channels affects the flow and heat transfer characteristics of minichannel heat sinks. The three-dimensional governing equations in steady state and laminar flow are solved using Finite Volume Method (FVM) with the SIMPLE algorithm. The results show that the numerical simulation is in good agreement with the experimental data. The thermal and hydrodynamic characteristics of the heat sinks including Nusselt number, friction factor, thermal resistance and pumping power for various geometries of heat sinks are discussed in details. The results indicate that the heat sink with rectangular cross-section has a better heat transfer rate and the circular channel heat sink has the lower pumping power.*

KEYWORDS: *Cooling performance; Computational Fluid Dynamics (CFD); Heat sink; Circular channel; Rectangular channel.*

INTRODUCTION

The heat sink is a type of heat exchanger utilized as a cooling system in electronic chips. The heat sink is used to increase the heat transfer area in electronic components, which is typically attached to the top of the electronic devices. The advantages of the heat sink are low initial cost, simple installation, and a reliable manufacturing process. In practical applications, the various sizes and shapes of heat sinks depend on the shape of the electronic device and available space for installation. Besides heat sinks, an important part of electronic cooling systems is the movement of fluid, where heat is transferred by air or water [1]. Thus, the characteristic of flow and heat transfer in the heat sink has become a very significant topic to attract more and more researchers' attention. The heat sink is typically made from a solid with high thermal conductivity such as

* *To whom correspondence should be addressed.*
+ *E-mail: s.ebrahim.ghasemi@stu.nit.ac.ir*
1021-9986/2018/2/231-239 9/$/5.09

silicon or copper. Over the past two decades, the need for removal of a large amount of heat from a small area, compactness and high heat transfer coefficient has attracted many researchers to study MicroChannel Heat Sinks (MCHSs). It is well known that when the passage size decreases, the heat transfer performance improves, at the expense of an increase in the pressure drop. Therefore, there is an optimum solution for the design of the MCHSs. Miniaturization of the heat sink is another technique to increase the cooling efficiency of the cooling system [2,3]. Numerical simulations of plate-circular pin-fin heat sinks in thermal and hydraulic performance were investigated by *Yang* an *Peng* [4]. The objective of their study was to examine the influence of the configurations of pin-fins design on the thermal resistance and the pressure drop of the heat sinks. *Conrad et al.* [5] investigated the performance of a pin fin heat sink that was directly attached to the chip. Their packaging concept exposed the chip directly to the cooling fluid. They concluded that plastic strain during operation can be significantly reduced compared to standard non-structured chip contacts. Furthermore, three-dimensional fluid flow and heat transfer phenomena inside heated microchannels were investigated by *Toh et al.* [6]. They solved the steady laminar flow and heat transfer equations using a finite-volume method. It was found that the heat input lowers the frictional losses and viscosity leading to an increase in the temperature of the water, particularly at lower Reynolds numbers. *Tiselj et al.* [7] performed experimental and numerical analysis of the effect of axial conduction on the heat transfer in triangular microchannel heat sink. They pointed out that the bulk water and heated wall temperatures did not change linearly along the channel. *Xie et al.* [8,9] investigate numerical studies on the laminar and turbulent flow and heat transfer characteristics of water-cooled straight microchannel heat sink. The effect of using nanofluid as working fluid on thermal performance of solar parabolic trough collector was investigated numerically [10-12]. *Ghasemi et al.* [13,14] proposed segmental rings for heat transfer enhancement of solar parabolic trough collector. The effects of segmental rings layouts on the heat transfer and system performance for non-uniform heat flux were discussed. The heat transfer and pressure drop characteristics of the parabolic solar collector with solid rings and porous rings were numerically studied using finite volume method by *Ghasemi and Ranjbar* [15,16]. An experimental database was compiled in order to fingerprint the scales formed over the hot surfaces of heat exchangers, in cooling water systems or other systems with similar chemistry by *Kameli et al*. [17]. *Mohebbi et al.* [18] investigated the convection heat transfer of Al_2O_3-water nanofluid turbulent flow through internally ribbed tubes with different rib shapes (rectangular, trapezoidal and semi-circular) numerically. The effect of CuO nanoparticles in distilled water on heat dissipation from electronic components was investigated numerically by *Ghasemi et al.* [19]. They used Computational Fluid Dynamics (CFD) simulations to study the rectangular and circular cross-sectional shaped heat sinks. Also, the thermal performance of a triangular shaped minichannel heat sink heat sink using alumina-water nanofluid as a coolant with different volume fractions was examined by *Ghasemi et al.* [20]. They concluded that when the volume fraction of nanoparticles increases under the extreme heat flux, the thermal resistance of the heat sink reduces. An experimental investigation on cooling performance of using nanofluid to replace the pure water as the coolant in a minichannel heat sink was conducted by *Ghasemi et al.* [21]. The experimental results showed that the nanofluid cooled heat sink outperforms the water-cooled one, having a significantly higher average heat transfer coefficient. Recently, *Ghasemi et al*. [22] investigated the cooling performance of heat sinks with a different hydraulic diameter of channel experimentally. They concluded that the heat transfer coefficient obtained from minichannel heat sink with D=4 mm is higher than that obtained from the minichannel heat sink with D= 6 mm and D=8 mm.

The main objective of this paper is to numerically study the thermo-hydraulic characteristics of rectangular and circular cross-sectional shaped heat sinks. Furthermore, the numerical results are compared with experimental data [22], and validation of the method is investigated.

THEORETICAL SECTION

Mathematical modeling is a vantage point to reach a solution in an engineering problem, so the accurate modeling of engineering problems is an important step to obtain accurate solutions [23–27]. Fig. 1 shows

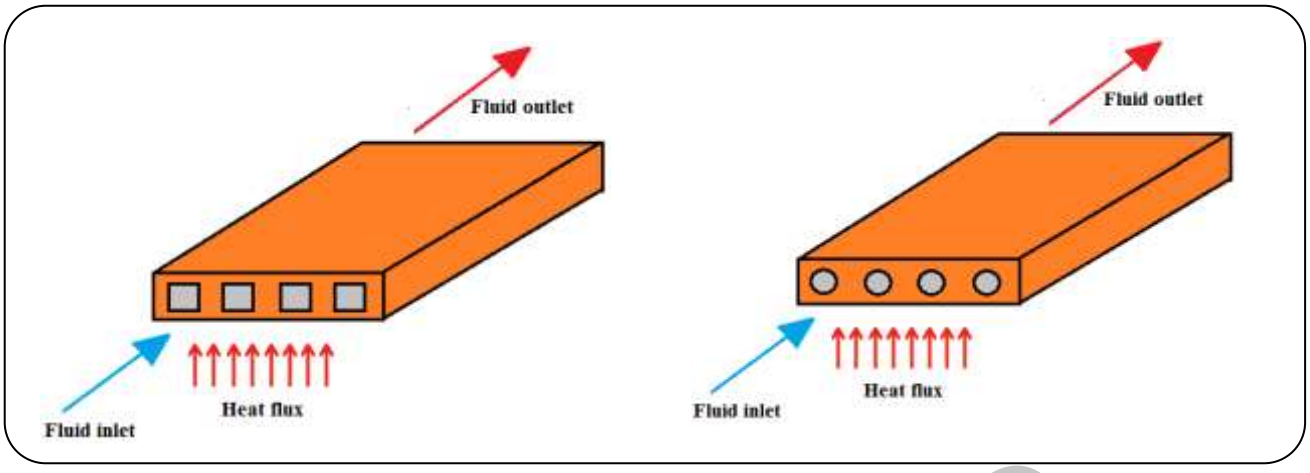

Fig. 1: Schematic of the heat sink with: a)rectangular channels and b)circular channels.

the schematic of the rectangular and circular heat sinks studied in the present work. Heat sink with the length and width of 50 mm and a total height of 15 mm is simulated. In this study, the thermal performances of two different heat sinks with rectangular and circular cross-sections using water as heat transfer fluid are studied numerically to investigate the effect of geometry of heat sink. The comparison is based on equal hydraulic diameter (D_h) and equal Reynolds number (Re), for both shapes. In order to simulate the heat generation in electronic chips, a uniform wall heat flux is applied on the bottom wall where the heat-generating chips are attached.

Governing equations

To numerical study on the effect of channel geometry on the heat sink performance, the governing continuity, momentum, and energy equations can be written as follows for incompressible, laminar and steady-state fluid flow [28]:

Continuity equation:

$$\frac{\partial u}{\partial x}+\frac{\partial v}{\partial y}+\frac{\partial w}{\partial z}=0 \quad (1)$$

Where *u*, *v*, and *w* are the velocity components in the x, y, and z directions, respectively.

Momentum equation:

$$\rho_f\left(u\frac{\partial u}{\partial x}+v\frac{\partial u}{\partial y}+w\frac{\partial u}{\partial z}\right)= \quad (2)$$
$$-\frac{\partial p}{\partial x}+\mu_f\left(\frac{\partial^2 u}{\partial x^2}+\frac{\partial^2 u}{\partial y^2}+\frac{\partial^2 u}{\partial z^2}\right)$$

$$\rho_f\left(u\frac{\partial v}{\partial x}+v\frac{\partial v}{\partial y}+w\frac{\partial v}{\partial z}\right)= \quad (3)$$
$$-\frac{\partial p}{\partial y}+\mu_f\left(\frac{\partial^2 v}{\partial x^2}+\frac{\partial^2 v}{\partial y^2}+\frac{\partial^2 v}{\partial z^2}\right)$$

$$\rho_f\left(u\frac{\partial w}{\partial x}+v\frac{\partial w}{\partial y}+w\frac{\partial w}{\partial z}\right)= \quad (4)$$
$$-\frac{\partial p}{\partial z}+\mu_f\left(\frac{\partial^2 w}{\partial x^2}+\frac{\partial^2 w}{\partial y^2}+\frac{\partial^2 w}{\partial z^2}\right)$$

Where ρ_f and μ_f are the density and dynamic viscosity of the coolant, respectively, and p is the coolant pressure.

Energy equation for the coolant:

$$\rho_f C_{p,f}\left(u\frac{\partial T_f}{\partial x}+v\frac{\partial T_f}{\partial y}+w\frac{\partial T_f}{\partial z}\right)= \quad (5)$$
$$k_f\left(\frac{\partial^2 T_f}{\partial x^2}+\frac{\partial^2 T_f}{\partial y^2}+\frac{\partial^2 T_f}{\partial z^2}\right)$$

Where T_f is the coolant's temperature, $C_{p,f}$ is its specific heat, and k_f is its thermal conductivity.

Energy equation for the solid region:

$$k_s\left(\frac{\partial^2 T_s}{\partial x^2}+\frac{\partial^2 T_s}{\partial y^2}+\frac{\partial^2 T_s}{\partial z^2}\right)=0 \quad (6)$$

Where T_s is the solid temperature, and k_s is the thermal conductivity of the solid.

In this study, pure water is to be used as the working fluid. The thermo physical properties of pure water are listed in Table 1.

Table 1: Thermo-physical properties of pure water.

	$\rho(kg/m^3)$	$C_p(J/kg.K)$	k(W/m.K)	$\mu(N.s/m^2)$
Pure water	997.1	4179	0.613	0.001003

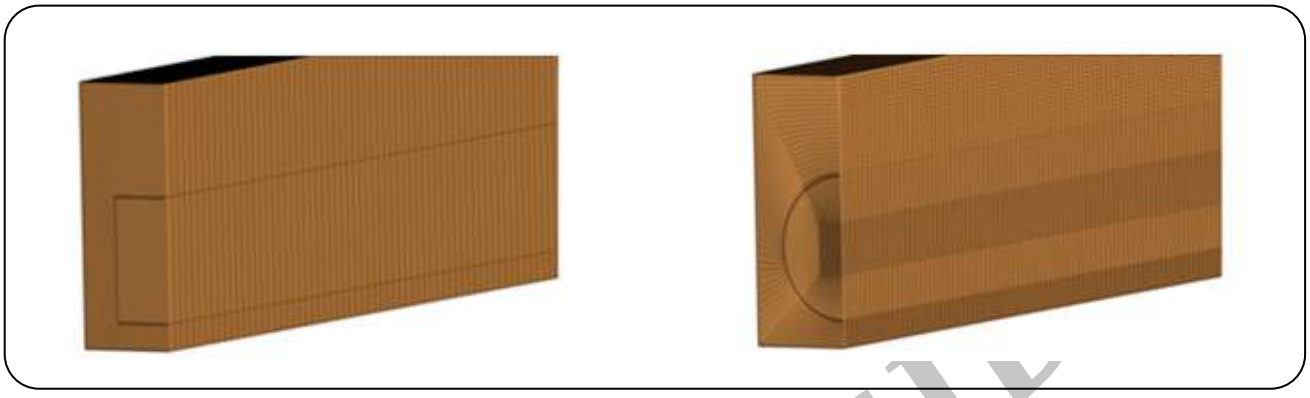

Fig. 2: Grid generation for the heat sink with: a)rectangular channels and b)circular channels.

Boundary conditions

Fluid enters the channel at the inlet with the same uniform axial velocity that is specified according to the Reynolds numbers. The no-slip boundary condition at the walls is appropriate for this study. For thermal boundary conditions, it is assumed that the fluid enters the channel with a constant temperature and also a constant heat flux is applied from the bottom, while the top glass layer is considered adiabatic. For the channel outlet, the outflow boundary condition is considered.

Numerical procedure

The geometrical model is created and meshed using commercial software GAMBIT. In order to reduce the number of grid cells and cut down the computational time, only one channel is modeled and studied. Fig. 2 shows the geometry of the grid of heat sinks for the circular and rectangular cross-section. In order to simplify the mesh generation and cut down computational time for the geometry of circular and rectangular cross-section, only one half of the computational domain is considered.

The governing equations are solved using the finite volume method with CFD commercial software ANSYS FLUENT [29]. The discretization scheme used for pressure is standard. The solution is based on pressure correction method and uses the SIMPLE algorithm. The second order upwind differencing scheme is used for momentum and energy equations. The solution is considered to be converged sufficiently when the normalized residual of 10^{-5} for momentum and mass and 10^{-8} for energy equations.

Grid independence study

In order to ensure that the numerical results are accurate, a grid independence study has been carried out. To find the most suitable size of mesh, grid independent test is performed for four grids (257950, 698970, 1227630, 1762610 cells). The Nusselt number has been estimated for each grid system and results are compared. Comparison of the results in Table 2 shows that the grid with 1227630 mesh cells is found sufficient for the current study.

Model validation

To check the validity of the built numerical model, verification is made by comparing current numerical results with experimental data of *Ghasemi et al.* [22]. In experimental work of *Ghasemi et al.* [22], four circular minichannels was used as a heat sink. The minichannel with the dimensions of 60 mm × 60 mm × 16 mm was fabricated and the heat transfer performances of a rectangular minichannel heat sink were investigated. Fig. 3 compares the experimental and the numerical simulation results for heat transfer coefficient and pressure drop. Numerical results show a higher heat transfer coefficient than the experimental results. For both the experimental and numerical results, the heat transfer coefficient

Table 2: Grid independence examination.

Grid system	Mesh cells	Nu	Nu-difference (%)
Grid 1	257950	1.77305	2.23 %
Grid 2	698970	1.81270	1.42 %
Grid 3	1227630	1.83845	0.11 %
Grid 4	1762610	1.84057	Baseline

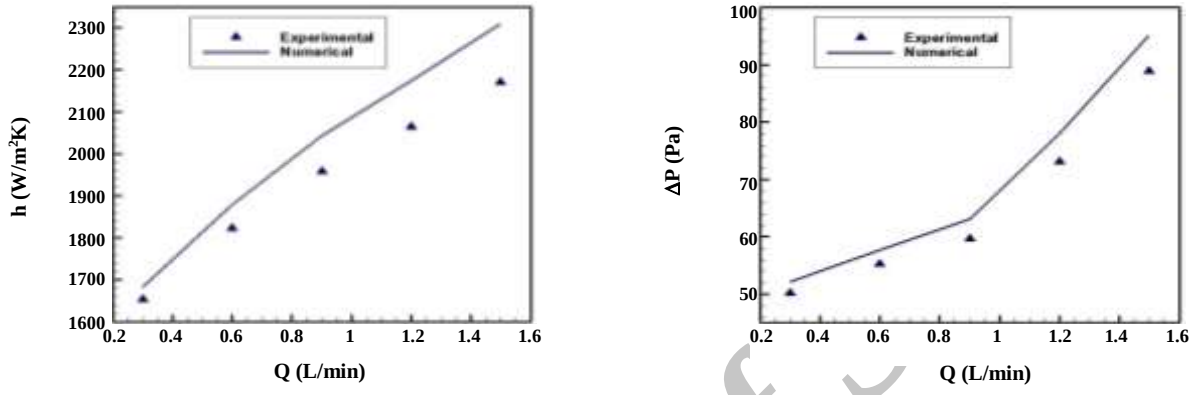

Fig. 3: Validation of the present numerical code with the experimental data of Ghasemi et al. [22] for: a) heat transfer coefficient and b) pressure drop.

increases with an increase in volume flow rate. According to Fig.3a, the maximum deviation of numerical simulation from the experimental results for the heat transfer coefficient is 6.4%. Also, for pressure drop (Fig.3b) this deviations is 7%. It can be seen that the numerical simulation results are in good agreement with the experimental data. Therefore the present numerical model is reliable and can be used to study the performance of a minichannel heat sink.

The average heat transfer coefficient (h_{ave}) has been calculated as follows:

$$h_{ave} = \frac{q''}{T_w - T_f} \tag{7}$$

Where q'' and T_w are heat flux and wall temperature respectively, and T_f is defined as:

$$T_f = \frac{T_{inlet} + T_{outlet}}{2} \tag{8}$$

RESULTS AND DISCUSSION

In this paper, to obtain the thermal performance of the rectangular and circular channel heat sinks, the numerical simulations of the fluid flow are evaluated. So, the thermal and hydrodynamic characteristics of the rectangular and circular heat sinks including Nusselt number, thermal resistance, friction factor, and pumping power for various Reynolds number are presented and discussed in details. Fig. 4 shows the average Nusselt numbers as a function of Reynolds number for rectangular and circular heat sinks. Reynolds number is defined as:

$$Re = \frac{\rho u D_h}{\mu} \tag{9}$$

Where ρ is the fluid density, u is the average velocity of the fluid at the inlet of the channel, D_h is the hydraulic diameter and μ is the dynamic viscosity.

The average Nusselt number is calculated by:

$$Nu = \frac{h_{ave} D_h}{k} \tag{10}$$

It can be seen in Fig. 4, the Nusselt number increases with an increase in Reynolds number for both cases. This means that a high inlet velocity is able to improve the cooling performance of the heat sinks. Furthermore,

it can be found that the heat sink with rectangular cross-section has a higher Nusselt number. It is because of that for the heat sink with rectangle cross-section, the ratio of surface area to cross-sectional area is greater and thus the rate of heat transfer for this case is more than the circular model.

Fig. 5 demonstrates the variant of friction factor versus Reynolds number for the heat sink with rectangular and circular cross-sections. The dimensionless friction factor through the heat sink is defined as [30]:

$$f = \frac{2D_h \Delta p}{\rho u^2 L} \quad (11)$$

Where D_h is the hydraulic diameter, Δp is the pressure drop of working fluid between inlet and outlet, ρ is the density of the fluid, u is the inlet velocity of the fluid, and L is the length of the channel.

As seen in Fig. 5, the friction factor of fluid in rectangular and circular cross-sections decreases with increasing Reynolds number because the friction factor and velocity have an inverse relationship therefore the friction factor reduced by increasing the Reynolds number. Also, it is concluded that for the case with a rectangular cross-section, the friction factor becomes higher at the same inlet Reynolds number.

As an important evaluation criterion of the thermal performance of heat sinks, the overall thermal resistance is defined as:

$$R_{th} = \frac{T_{max} - T_{in}}{q_{in}} \quad (12)$$

Where T_{max} is the maximum temperature of the wall at the fluid-solid interface of the bottom channel, and T_{in} is the coolant inlet temperature. Also, q_{in} is total power generated by the chip.

Fig. 6 presents the relationship between the Reynolds number and the thermal resistance rectangular and circular heat sinks respectively.

From the figure, it is seen that the higher Reynolds number represents the lower thermal resistance for both heat sinks. Improvement in thermal transportation increases the convective heat transfer coefficient that is inversely related to the convective thermal resistance. So, the enhancing in convective heat transfer coefficient ultimately decreases the thermal resistance of the nanofluid. Furthermore, it can be found that the thermal the resistance

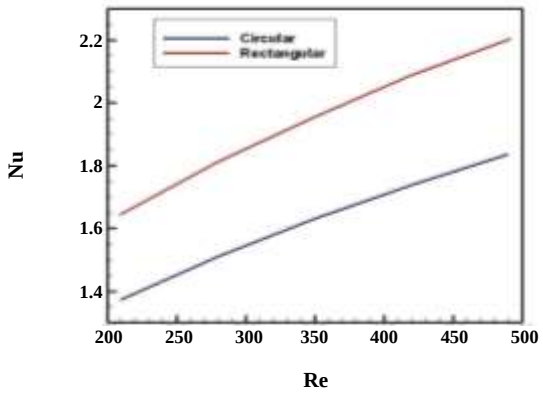

Fig. 4: Nusselt number versus Reynolds number for rectangular and circular channels.

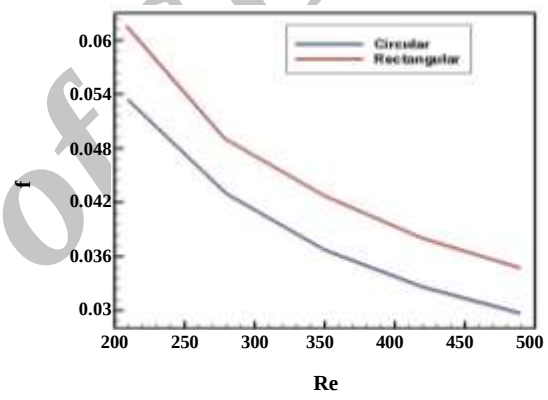

Fig. 5: Friction factor versus Reynolds number for rectangular and circular channels.

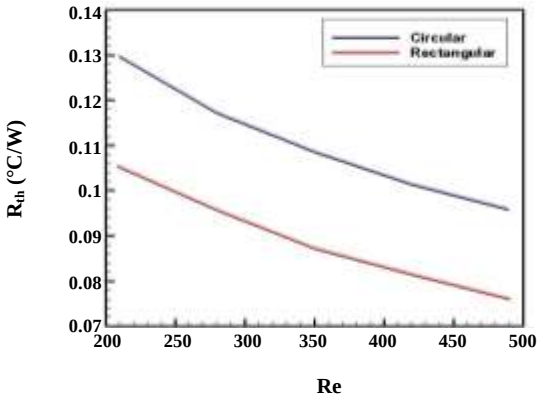

Fig. 6: Thermal resistance versus Reynolds number for rectangular and circular channels.

of the heat sink with the rectangular cross-section is obviously lower than that of the circular one.

When the coolant passes through the channel of the heat sink, a pressure drop occurs. So, to overcome this pressure drop, the system needs some extra pumping power. The Pumping Power (PP) is given by:

$$PP = \Delta p.Q \quad (13)$$

Where Δp is pressure drop across the heat sink and Q is volume flow rate. Fig. 7 presents the pumping power of heat sink versus Reynolds number for two different geometry of channels. It is evident that the heat sink with distilled water has the lower pumping power in comparison with the nanofluid for both of geometry. Fig. 7 demonstrates that the pumping power increases with the increase of the Reynolds number, owing to that with the increase of the inlet flow rate, the pressure drop enhances so more power is needed for pumping. It is obvious from this figure that the heat sink with circular cross-section has the lower pumping lower in comparison with the other case.

The temperature distribution of the outlet section of the heat sink for two different geometry of the channel is demonstrated in Fig. 8. This figure shows that the thermal transportation of the fluid for the rectangular channel is higher than the circular channel. The convective thermal resistance is inversely related to the convective heat transfer coefficient. So, the lower thermal resistance of the nanofluid for rectangular channel represents the improvement of the convective heat transportation capacity of the coolant and better reduction of the base temperature of the rectangular heat sink in comparison with circular one.

Fig. 9 presents the temperature distribution along the channel at the same Reynolds number for two different geometry of heat sink. It is seen that for the heat sink with the rectangular cross-section, the heat dissipation is larger in comparison with other which is due to the lower thermal resistance of this case.

CONCLUSIONS

In the current study, laminar forced convection heat transfer in the rectangular and circular mini channel heat sinks was simulated, and the heat transfer and pressure drop characteristics were analyzed for various Reynolds number. The finite volume approach was utilized for

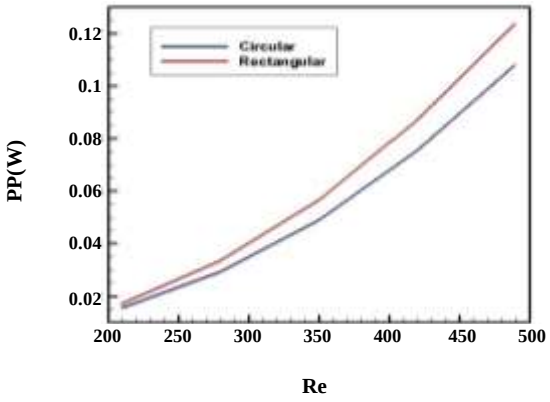

Fig. 7: Pumping power versus Reynolds number for rectangular and circular channels.

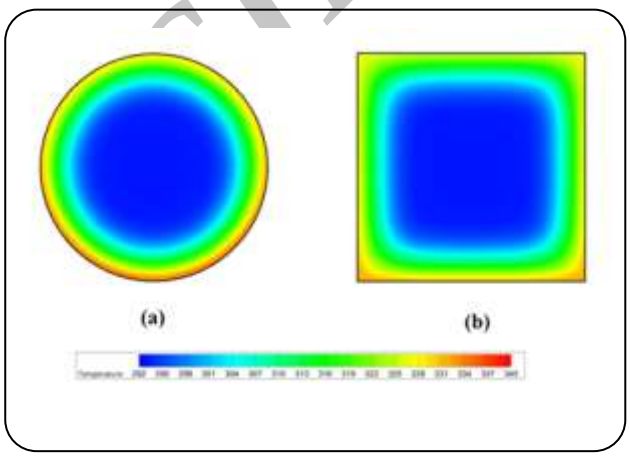

Fig. 8: Temperature distributions on the heated bottom wall of the heat sink with: a) circular channels, b) rectangular channels.

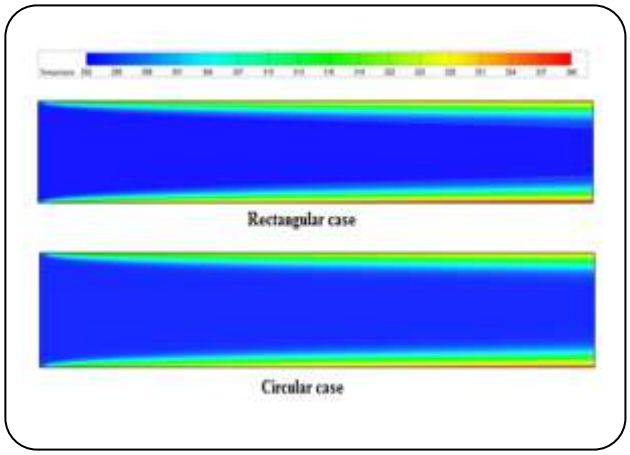

Fig. 9: Temperature distributions for a heat sink with rectangular and circular cross-sections.

solving the incompressible, three dimensional and steady-state problem. The validation was done to compare the numerical results with the experimental data. The effects of different geometry of channel on the thermo-hydraulic behavior of the heat sink were investigated. As a first result, the numerical results were in a good agreement with experimental data. On the basis of equal hydraulic diameter and equal Reynolds number, the heat sink with rectangular channels has less thermal resistance but requires more pumping power than heat sink with circular channels. Also, the results showed that the friction factor decreases with increasing Reynolds number.

Nomenclature

$\vec{V}$	Velocity vector
Re	Reynolds number
ρ	Density
u	Average velocity
p	Pressure
D_h	Hydraulic diameter
C_p	Specific heat
h	Heat transfer coefficient
k	Thermal conductivity
μ	Viscosity
f	Friction factor
T	Temperature
Nu	Nusselt number
q"	Heat flux
PP	Pumping power
R_{th}	Thermal resistance
q_{in}	Total heating power
Q	Volume flow rate
L	Channel length

Received: Jun. 7, 2016; Accepted: Jul. 17, 2017

REFERENCES

[1] Chingulpitak S., Wongwises S., A Review of the Effect of Flow Directions and Behaviors on the Thermal Performance of Conventional Heat Sinks, *Int. J. Heat Mass Transfer*, **81**: 10-18 (2015).

[2] Kuppusamy N.R., Mohammed H.A., Lim C.W., Numerical Investigation of Trapezoidal Grooved Microchannel Heat Sink Using Nanofluids, *Thermochim. Acta*, **573**: 39-56 (2013).

[3] Salman B., Mohammed H.A., Munisamy K.M., Kherbeet A.Sh., Characteristics of Heat Transfer and Fluid Flow in Microtube and Microchannel Using Conventional Fluids and Nanofluids: a Review, *Renew. Sustainable Energy Rev.*, **28**: 848-880 (2013).

[4] Yang Yue-Tzu, Peng Huan-Sen, Investigation of Planted Pin Fins for Heat Transfer Enhancement in Plate Fin Heat Sink, *Microelectron. Reliab.*, **49**: 163–169 (2009).

[5] Conrad M., Diatlov A., De Doncker R.W., Purpose, Potential and Realization of Chip Attached Micro-Pin Fin Heat Sinks, *Microelectron. Reliab.*, **55:** 1992–1996 (2015).

[6] Toh K.C., Chen X.Y., Chai J.C., Numerical Computation of Fluid Flow and Heat Transfer in Microchannels, *Int. J. Heat Mass Transfer*, **45:** 5133–5141 (2002).

[7] Tiselj I., Hetsroni G., Mavko B., Mosyak A., Pogrebnyak E., Segal Z., Effect of Axial Conduction on the Heat Transfer in Microchannels, *Int. J. Heat Mass Transfer*, **47:** 2551–2565 (2004).

[8] Xie X.L., Liu Z.J., He Y.L., Tao W.Q., Numerical Study of Laminar Heat Transfer and Pressure Drop Characteristics in a Water-Cooled Minichannel Heat Sink, *Appl. Therm. Eng.*, **29:** 64–74 (2009).

[9] Xie X.L., Tao W.Q., He Y.L., Numerical Study of Turbulent Heat Transfer and Pressure Drop Characteristics in a Water-cooled Minichannel Heat Sink, *ASME J. Electron. Packag.*, **129:** 247–255 (2007).

[10] Ghasemi S.E., Ranjbar A.A., Ramiar A., Numerical Investigation of Effect of Al-water Nanofluid on Performance of Solar Parabolic Collector, *Nanomaterials*, **14**(5): 100-107 (2013).

[11] Ghasemi S.E., Ranjbar A.A., Thermal Performance Analysis of Solar Parabolic Trough Collector Using Nanofluid Asworking Fluid: A CFD Modelling Study, *J. Mol. Liq.*, **222:** 159–166 (2016).

[12] Ghasemi S.E., Ranjbar A.A., Effect of Using Nanofluids on Efficiency of Parabolic Trough Collectors in Solar Thermal Electric Power Plants, *Int. J. Hydrogen Energy*, http://dx.doi.org/10.1016/j.ijhydene.2017.07.087.

[13] Ghasemi S.E., Ranjbar A.A., Ramiar A., Three-Dimensional Numerical Analysis of Heat Transfer Characteristics of Solar Parabolic Collector with Two Segmental Rings, *J. Math. Comput. Sci.*, **7**:89–100 (2013).

[14] Ghasemi S.E., Ranjbar A.A., Ramiar A., Numerical Study on Thermal Performance of Solar Parabolic Trough Collector, *J. Math. Comput. Sci*.,**7**:1–12 (2013).

[15] Ghasemi Seyed Ebrahim, Ranjbar Ali Akbar, Thermal Efficiency Evaluation of Solar Rings in Tubes, *Eur. Phys. J. Plus*., **131**: 430 (2016).

[16] Ghasemi Seyed Ebrahim, Ranjbar Ali Akbar, Numerical Thermal Study on Effect of Porous Rings on Performance of Solar Parabolic Trough Collector, *Appl. Therm. Eng*., **118:** 807–816 (2017).

[17] Kameli M., Esmaeili N., Rahimi Mofrad H., Diagnosis of Heat Exchanger Scales in Cooling Water Systems, *Iran. J. Chem. Chem. Eng. (IJCCE)*, **27**(1): 65-71 (2008).

[18] Mohebbi K., Rafee R., Talebi F., Effects of Rib Shapes on Heat Transfer Characteristics of Turbulent Flow of Al2O3-Water Nanofluid inside Ribbed Tubes, *Iran. J. Chem. Chem. Eng. (IJCCE)*, **34**(3): 61-77 (2015).

[19] Ghasemi Seyed Ebrahim, Ranjbar A.A., Hosseini M.J., Numerical Study on Effect of CuO-Water Nanofluid on Cooling Performance of Two Different Cross-Sectional Heat Sinks, *Adv. Powder Technol*., **28:** 1495–1504 (2017).

[20] Ghasemi Seyed Ebrahim, Ranjbar A.A., Hosseini M.J., Thermal and Hydrodynamic Characteristics of Water-Based Suspensions of Al_2O_3 Nanoparticles in a Novel Minichannel Heat Sink, *J. Mol. Liq*., **230:** 550–556 (2017).

[21] Ghasemi Seyed Ebrahim, Ranjbar A.A., Hosseini M.J., Experimental Evaluation of Cooling Performance of Circular Heat Sinks for Heat Dissipation from Electronic Chips Using Nanofluid, Mechanics Research Communications, *Mech Res Commun*., **84:** 85–89 (2017).

[22] Ghasemi Seyed Ebrahim, Ranjbar A.A., Hosseini M.J., Experimental and Numerical Investigation of Circular Minichannel Heat Sinks with Various Hydraulic Diameter for Electronic Cooling Application, *Microelectron. Reliab.*, **73:** 97–105 (2017).

[23] Bahramian A.R., Kalbasi M., CFD Modeling of TiO_2 Nano-Agglomerates Hydrodynamics in a Conical Fluidized Bed Unit with Experimental Validation, *Iran. J. Chem. Chem. Eng. (IJCCE)*, **29**(2): 105-120 (2010).

[24] Abdoli Rad M., Shahsavand A., Modeling and Simulation of Heat Transfer Phenomenon in Steel Belt Conveyer Sulfur Granulating Process, *Iran. J. Chem. Chem. Eng. (IJCCE)*, **32**(4): 93-104 (2013).

[25] Wadhwani R., Mohanty B., Computational Fluid Dynamics Study of a Complete Coal Direct Chemical Looping Sub-Pilot Unit, *Iran. J. Chem. Chem. Eng. (IJCCE)*, **35**(3): 139-153 (2016).

[26] Jafari A., Shahmohammadi A., Mousavi S.M., CFD Investigation of Gravitational Sedimentation Effect on Heat Transfer of a Nano-Ferrofluid, *Iran. J. Chem. Chem. Eng. (IJCCE)*, **34**(1): 87-96 (2015).

[27] Sarrami Foroushani Ali, Nasr Esfahany Mohsen, CFD Simulation of Gas-Solid Two-Phase Flow in Pneumatic Conveying of Wheat, *Iran. J. Chem. Chem. Eng. (IJCCE)*, **34**(4): 123-140 (2015).

[28] Patankar S.V., "Numerical Heat Transfer and Fluid Flow", Hemisphere, New York (1980).

[29] Fluent Inc. FLUENT 6.3 User's Guide. Fluent Publishing Company, Lebanon (2007).

[30] Moody L.F., Friction Factors For Pipe Flow, *J. Heat Transfer*, **66** (8): 671–684 (1944).